

# Analysis of Galactic Rotation from Masers Based on a Nonlinear Oort Model

V.V. Bobylev<sup>1,2 0</sup>, A.T.Bajkova<sup>1</sup>

<sup>1</sup>*Pulkovo Astronomical Observatory, Russian Academy of Sciences,  
Pulkovskoe sh. 65, St. Petersburg, 196140 Russia*

<sup>2</sup>*Sobolev Astronomical Institute, St. Petersburg State University,  
Universitetskii pr. 28, Petrodvorets, 198504 Russia*

Based on data on Galactic masers with measured trigonometric parallaxes, we have tested a nonlinear model of Galactic rotation using generalized Oort formulas. This model is shown to yield pretty good results up to heliocentric distances of 3–4 kpc. The main feature of the method is the possibility of estimating the solar Galactocentric distance  $R_0$ . This distance has been found by analyzing  $\approx 60$  masers to be  $R_0 = 8.3 \pm 0.4$  kpc. Our study of the three-dimensional kinematics of more than 100 masers based on the Ogorodnikov–Milne model has shown that significant nonlinearities are present only in the  $xy$  plane (rotation around the Galactic  $z$  axis) due to the peculiarities of the Galactic rotation curve. No significant linear dependences have been found in the  $xz$  and  $yz$  planes. We show the presence of a wave in the velocities  $w$  as a function of coordinate  $x$  or distance  $R$  with a wavelength of 3 kpc and an amplitude of  $10 \text{ km s}^{-1}$ . The wave is particularly prominent in the Local and Perseus arms.

**DOI:** 10.1134/S1063773714120019

Keywords: *kinematics, masers, Galaxy.*

arXiv:1411.2508v1 [astro-ph.GA] 10 Nov 2014

---

<sup>0</sup>e-mail: vbobylev@gao.spb.ru

# INTRODUCTION

The parameters of Galactic rotation have been repeatedly determined by many authors using objects belonging to various structural components of the Galaxy: from ionized and neutral hydrogen (Clemens 1985; McClure-Griffiths and Dickey 2007; Levine et al. 2008), from distant OB associations (Mel'nik and Dambis 2009), and from open star clusters (Zabolot'skikh et al. 2002; Popova and Loktin 2005; Bobylev et al. 2007). Galactic masers are of great interest for studying the Galactic kinematics, because their trigonometric parallaxes are measured by VLBI with a high accuracy, on average, at least 10% (Reid et al. 2014).

One of the important problems is to determine the Galactocentric distance of the Sun  $R_0$ . Reid (1993) published a review of the  $R_0$  measurements made by then by various methods. He divided all measurements into primary, secondary, and indirect ones and obtained the “best value” as a weighted mean of the published measurements over a period of 20 years:  $R_0 = 8.0 \pm 0.5$  kpc. Nikiforov (2003) proposed a more complete three-dimensional classification in which the type of  $R_0$  determination method, the method of finding the reference distances, and the type of reference objects are taken into account. Taking into account the main types of errors and correlations associated with the classes of measurements, he obtained the “best value”  $R_0 = 7.9 \pm 0.2$  kpc by analyzing the results of various authors published between 1974 and 2003. Based on the results published between 1992 and 2010, Foster and Cooper (2010) obtained the mean  $R_0 = 8.0 \pm 0.4$  kpc. Since the scatter of individual estimates is significant, applying independent methods is of great interest.

The direct methods of determining the distance  $R_0$  are not all that many. These include such methods as the VLBI measurements of the trigonometric parallaxes for masers at the Galactic center, the use of Cepheids and globular clusters, or the application of the dynamical parallax method to analyze the motion of stars around the supermassive central black hole. There are much more indirect methods. The various kinematic methods of estimating  $R_0$  occupy an important place among them. In particular, using such a method, Reid et al. (2014) obtained an estimate of  $R_0 = 8.34 \pm 0.16$  kpc by analyzing the kinematics of Galactic masers, while Bobylev and Bajkova (2014) found  $R_0 = 8.3 \pm 0.2$  kpc from masers, with these authors having applied different methods of analysis.

The number of masers with measured trigonometric parallaxes already exceeds 100. This allows one not only to study the Galactic rotation parameters and the influence of the spiral structure (the  $xy$  plane) but also to check the presence of some kinematic peculiarities in the other two planes ( $xz$  and  $yz$ ). Such a check is one of the goals of this paper. For example, a kinematic relationship to the Galactic warp (Bobylev 2013), which manifests itself in the  $yz$  plane, is revealed in the motion of distant Cepheids. Having analyzed OB stars, Branham (2014) found significantly nonzero values of the gradients  $\partial w / \partial z$  and  $\partial^2 w / \partial^2 z$ . He used a nonlinear model based on generalized Oort formulas, which served as a stimulus for applying a similar approach in this paper. Vityazev and Tsvetkov (2014) reported the existence of significantly nonzero beyond-the-model (with respect to the linear Ogorodnikov-Milne model) harmonics in the motion of stars from various catalogs.

The main goal of this paper is to test a nonlinear model of Galactic rotation using generalized Oort formulas. Such an approach allows the angular velocity of Galactic rotation and its derivatives as well as the solar Galactocentric distance  $R_0$  to be estimated.

# DATA

Based on published data, we gathered information about the coordinates, line-of-sight velocities, proper motions, and trigonometric parallaxes of Galactic masers measured by VLBI with an error, on average, less than 10%. These masers are associated with very young objects, protostars of mostly high masses located in regions of active star formation. The proper motions and trigonometric parallaxes of the masers are absolute, because they are determined with respect to extragalactic reference objects (quasars).

One of the projects to measure the trigonometric parallaxes and proper motions is the Japanese VERA (VLBI Exploration of Radio Astrometry) project devoted to the observations of H<sub>2</sub>O masers at 22.2 GHz (Hirota et al. 2007) and a number of SiO masers (which are very few among young objects) at 43 GHz (Kim et al. 2008).

Methanol (CH<sub>3</sub>OH, 6.7 and 12.2 GHz) and H<sub>2</sub>O masers are observed in the USA on VLBA (Reid et al. 2009a). Similar observations are also being carried out within the framework of the European VLBI network (Rygl et al. 2010), in which three Russian antennas are involved: Svetloe, Zelenchukskaya, and Badary. These two programs enter into the BeSSeL project<sup>1</sup> (Bar and Spiral Structure Legacy Survey, Brunthaler et al. 2011).<sup>1</sup>

The VLBI observations of radio stars in continuum at 8.4 GHz are being carried out with the same goals (Torres et al. 2009; Dzib et al. 2011). Radio sources located in the local (Orion) arm associated with young low-mass protostars are observed within the framework of this program.

Our sample includes a total of 117 sources. In addition to 103 masers from Reid et al. (2014), it includes 14 more sources whose trigonometric parallaxes have been measured by VLBI:

(1) the high-mass spectroscopic binary Cyg X-1 (Reid et al. 2011), with one of its components being a black hole candidate, we took the line-of-sight velocity for this binary  $V_\gamma$  from Ziolkowski (2005);

(2) the red supergiant IRAS 22480+6002 (Imai et al. 2012);

(3) the red supergiant PZ Cas (Kusuno et al. 2013);

(4) the source SVS 13 in NGC 1333 (Hirota et al. 2008), with the data having been averaged over two features, f1 and f2;

(5–9) five low-mass nearby radio stars in Taurus: Hubble 4 and HDE 283572 (Torres et al. 2007), T Tau N (Loinard et al. 2007), HP Tau/G2 (Torres et al. 2009), and V773 Tau (Torres et al. 2012);

(10–12) three radio stars: S1 and DoAr21 (Loinard et al. 2008) as well as EC 95 (Dzib et al. 2010) with their line-of-sight velocities  $V_{LSR}$  from Honma et al. (2012);

(13) IRAS 20143+3634 (Burns et al. 2014);

(14) IRAS 22555+6213 (Chibueze et al. 2014).

Note that we took a new estimate of the distance and proper motion for the star-forming region S 269 (which enters into the sample of 103 masers) from Asaki et al. (2014).

# METHODS

Here, we use a rectangular Galactic coordinate system with the axes directed away from the observer toward the Galactic center ( $l=0^\circ$ ,  $b=0^\circ$ , the  $x$  axis), in the direction of Galactic

---

<sup>1</sup><http://www3.mpifr-bonn.mpg.de/staff/abrunthaler/BeSSeL/index.shtml>

rotation ( $l=90^\circ$ ,  $b=0^\circ$ , the  $y$  axis), and toward the north Galactic pole ( $b=90^\circ$ , the  $z$  axis).

## Generalized Oort Equations

Bottlinger's equations are

$$\begin{aligned} V_r &= -(\omega - \omega_0)R_0 \sin l \cos b, \\ V_l &= -(\omega - \omega_0)R_0 \cos l + \omega r \cos b, \\ V_b &= (\omega - \omega_0)R_0 \sin l \sin b, \end{aligned} \quad (1)$$

where the signs at the angular velocities of Galactic rotation  $\omega$  and  $\omega_0$  correspond to positive rotation from the  $x$  axis to  $y$ , i.e., counterclockwise rotation. The angular velocity  $\omega$  is then expanded in a series to terms of the second order in  $r/R_0$ . In this case, the distance from the star to the Galactic rotation axis  $R$ ,

$$\begin{aligned} R^2 &= r^2 \cos^2 b - \\ &- 2R_0 r \cos b \cos l + R_0^2 \end{aligned} \quad (2)$$

is again expanded in a series in  $r/R_0$  and then only the first two expansion terms are used:  $R \approx R_0 - r \cos b \cos l$ . The resulting expressions are called the generalized Oort equations. They are written as (Ogorodnikov 1965)

$$\begin{aligned} V_r &= -u_\odot \cos b \cos l - v_\odot \cos b \sin l - \\ &- w_\odot \sin b + rA \cos^2 b \sin 2l - \\ &- r^2 F \cos^3 b \sin l \cos^2 l - \\ &- r^2 (A^\circ/R_0) \cos^3 b \sin^3 l, \end{aligned} \quad (3)$$

$$\begin{aligned} V_l &= u_\odot \sin l - v_\odot \cos l + \\ &+ rA \cos b \cos 2l + rB \cos b - \\ &- r^2 F \cos^2 b \cos^3 l - \\ &- r^2 (A^\circ/R_0) (3 \cos^2 b \cos l - \\ &- \cos^2 b \cos^3 l), \end{aligned} \quad (4)$$

$$\begin{aligned} V_b &= u_\odot \cos l \sin b + v_\odot \sin l \sin b - \\ &- w_\odot \cos b - rA \cos b \sin b \sin 2l + \\ &+ r^2 F \cos^2 b \sin b \sin l \cos^2 l + \\ &+ r^2 (A^\circ/R_0) \cos^2 b \sin b \sin^3 l, \end{aligned} \quad (5)$$

where  $V_r$  is the line-of-sight velocity of the star (in  $\text{km s}^{-1}$ );  $r = 1/\pi$  is the heliocentric distance of the star;  $V_l = 4.74r\mu_l \cos b$  and  $V_b = 4.74r\mu_b$  are the proper motion velocity components of the star (in  $\text{mas yr}^{-1}$ ) in the  $l$  and  $b$  directions, respectively; the coefficient 4.74 is the quotient of the number of kilometers in an astronomical unit by the number of seconds in a tropical year;  $u_\odot, v_\odot, w_\odot$  are the stellar group velocity components relative to the Sun taken with the opposite sign (the velocity  $u$  is directed toward the Galactic center,  $v$  is in the direction of Galactic rotation,  $w$  is directed to the north Galactic pole);  $R_0$  is the Galactocentric distance of the Sun;  $\omega_0$  is the angular velocity of rotation at the distance  $R_0$ ; the parameters  $\omega'_0$  and  $\omega''_0$  are the first and second derivatives of the angular velocity, respectively

The system of conditional equations (3)–(5) contains seven unknowns:  $u_\odot, v_\odot, w_\odot, A, B, F$  and  $A^\circ/R_0$ , which are determined by the least-squares method. Here,  $A$  and  $B$  denote

the Oort constants,  $A = 0.5R_0\omega'_0$  and  $B = 0.5R_0\omega'_0 + \omega_0$ , consequently,  $\omega_0 = B - A$ , while  $F$  denotes the second-order coefficient  $F = 0.5R_0\omega''_0$ .  $R_0$  is calculated using the values of  $A$  and  $A^\circ/R_0$  found as  $R_0 = A/(A^\circ/R_0)$ . The error in  $R_0$  is found from the relation  $\varepsilon(R_0) = \varepsilon(A)/(A^\circ/R_0)$ .

As a result, in addition to the peculiar solar velocity components  $u_\odot, v_\odot, w_\odot$ , the method allows the Galactic rotation parameters  $\omega_0$ ,  $\omega'_0$ , and  $\omega''_0$  and the distance  $R_0$  to be estimated irrespective of any a priori assumptions.

## The Linear Ogorodnikov–Milne Model

In the linear Ogorodnikov–Milne model (Ogorodnikov 1965), the observed velocity  $\mathbf{V}(r)$  of a star with a heliocentric radius vector  $\mathbf{r}$  is described, to terms of the first order of smallness  $r/R_0 \ll 1$ , by the vector equation

$$\mathbf{V}(r) = \mathbf{V}_\odot + M\mathbf{r} + \mathbf{V}'. \quad (6)$$

Here,  $\mathbf{V}_\odot(u_\odot, v_\odot, w_\odot)$  is the Sun’s peculiar velocity relative to the stars under consideration,  $\mathbf{V}'$  is the star’s residual velocity,  $M$  is the displacement matrix whose components are the partial derivatives of the velocity  $\mathbf{u}(u, v, w)$  with respect to the distance  $\mathbf{r}(x, y, z)$ , where  $\mathbf{u} = \mathbf{V}(R) - \mathbf{V}(R_0)$ . Neglecting the residual velocities, Eqs. (6) can be written in an expanded form as

$$\begin{aligned} u &= u_\odot + \left(\frac{\partial u}{\partial x}\right)_\circ x + \left(\frac{\partial u}{\partial y}\right)_\circ y + \left(\frac{\partial u}{\partial z}\right)_\circ z, \\ v &= v_\odot + \left(\frac{\partial v}{\partial x}\right)_\circ x + \left(\frac{\partial v}{\partial y}\right)_\circ y + \left(\frac{\partial v}{\partial z}\right)_\circ z, \\ w &= w_\odot + \left(\frac{\partial w}{\partial x}\right)_\circ x + \left(\frac{\partial w}{\partial y}\right)_\circ y + \left(\frac{\partial w}{\partial z}\right)_\circ z, \end{aligned} \quad (7)$$

where the subscript 0 means that the derivatives are taken at  $R = R_0$ . In cylindrical coordinates  $(R, \theta, z)$ , the displacement matrix  $M$  is

$$M = \begin{pmatrix} \frac{\partial V_R}{\partial R} & \frac{1}{R} \frac{\partial V_R}{\partial \theta} - \frac{V_\theta}{R} & \frac{\partial V_R}{\partial z} \\ \frac{\partial V_\theta}{\partial R} & \frac{1}{R} \frac{\partial V_\theta}{\partial \theta} + \frac{V_R}{R} & \frac{\partial V_\theta}{\partial z} \\ \frac{\partial V_z}{\partial R} & \frac{1}{R} \frac{\partial V_z}{\partial \theta} & \frac{\partial V_z}{\partial z} \end{pmatrix}. \quad (8)$$

Here, all derivatives are taken at the point with coordinates  $(R = R_\circ, \theta = 0^\circ, z = z_0)$ .

## RESULTS

Following the recommendations of Reid et al. (2014), we did not use any masers located at distances  $R < 4$  kpc when determining the Galactic rotation parameters, because the influence of the noncircular motions associated with the influence of the central Galactic bar is great in this region. To determine the Galactic rotation parameters, we produced a sample of “best” masers. For this purpose, we solved the system of equations (3)–(5) using the constraints  $\varepsilon_\pi/\pi \leq 10\%$  and  $r \leq 4$  kpc that are met by 66 masers. As a result of successive

rejections according to the  $3\sigma$  criterion, 60 sources remained. The following masers turned out to be the rejected ones: G012.68.00.18, G016.58.00.05, G034.39+00.22, G078.12+03.63, G078.88+00.70, and G108.59+00.49. As a result, we obtained the following solution:

$$\begin{aligned}
u_{\odot} &= 8.5 \pm 1.3 \text{ km s}^{-1}, \\
v_{\odot} &= 15.7 \pm 1.4 \text{ km s}^{-1}, \\
w_{\odot} &= 9.0 \pm 1.0 \text{ km s}^{-1}, \\
A &= 15.03 \pm 0.65 \text{ km s}^{-1} \text{ kpc}^{-1}, \\
B &= -14.94 \pm 0.69 \text{ km s}^{-1} \text{ kpc}^{-1}, \\
F &= -2.74 \pm 0.69 \text{ km s}^{-1} \text{ kpc}^{-2}, \\
A^{\circ}/R_0 &= 1.80 \pm 0.25 \text{ km s}^{-1} \text{ kpc}^{-2},
\end{aligned} \tag{9}$$

based on which we found

$$\begin{aligned}
\omega_0 &= -29.97 \pm 0.95 \text{ km s}^{-1} \text{ kpc}^{-1}, \\
\omega'_0 &= 3.59 \pm 0.16 \text{ km s}^{-1} \text{ kpc}^{-2}, \\
\omega''_0 &= -0.66 \pm 0.16 \text{ km s}^{-1} \text{ kpc}^{-3}, \\
R_0 &= 8.35 \pm 0.36 \text{ kpc}.
\end{aligned}$$

The error per unit weight is  $\sigma_0 = 7.9 \text{ km s}^{-1}$ , with solution (9) having been obtained with unit weights. In the case of applying a system of weights in the form  $w_r = S_0/\sqrt{S_0^2 + \sigma_{V_r}^2}$ ,  $w_l = S_0/\sqrt{S_0^2 + \sigma_{V_l}^2}$  and  $w_b = S_0/\sqrt{S_0^2 + \sigma_{V_b}^2}$ , where  $S_0$  denotes the ‘‘cosmic’’ dispersion taken to be  $8 \text{ km s}^{-1}$ , the solution is

$$\begin{aligned}
u_{\odot} &= 9.5 \pm 1.3 \text{ km s}^{-1}, \\
v_{\odot} &= 15.9 \pm 1.4 \text{ km s}^{-1}, \\
w_{\odot} &= 8.6 \pm 0.9 \text{ km s}^{-1}, \\
A &= 15.64 \pm 0.66 \text{ km s}^{-1} \text{ kpc}^{-1}, \\
B &= -15.29 \pm 0.73 \text{ km s}^{-1} \text{ kpc}^{-1}, \\
F &= -3.16 \pm 0.79 \text{ km s}^{-1} \text{ kpc}^{-2}, \\
A^{\circ}/R_0 &= 1.84 \pm 0.28 \text{ km s}^{-1} \text{ kpc}^{-2},
\end{aligned} \tag{10}$$

based on which we find

$$\begin{aligned}
\omega_0 &= -30.93 \pm 0.99 \text{ km s}^{-1} \text{ kpc}^{-1}, \\
\omega'_0 &= 3.68 \pm 0.16 \text{ km s}^{-1} \text{ kpc}^{-2}, \\
\omega''_0 &= -0.74 \pm 0.19 \text{ km s}^{-1} \text{ kpc}^{-3}, \\
R_0 &= 8.50 \pm 0.36 \text{ kpc},
\end{aligned}$$

with the error per unit weight being  $\sigma_0 = 7.6 \text{ km s}^{-1}$ . It can be seen that there are no significant differences from the solution with unit weights in this case.

Below, we give one more solution obtained under the constraints  $\varepsilon_{\pi}/\pi \leq 10\%$  and  $r \leq 3$

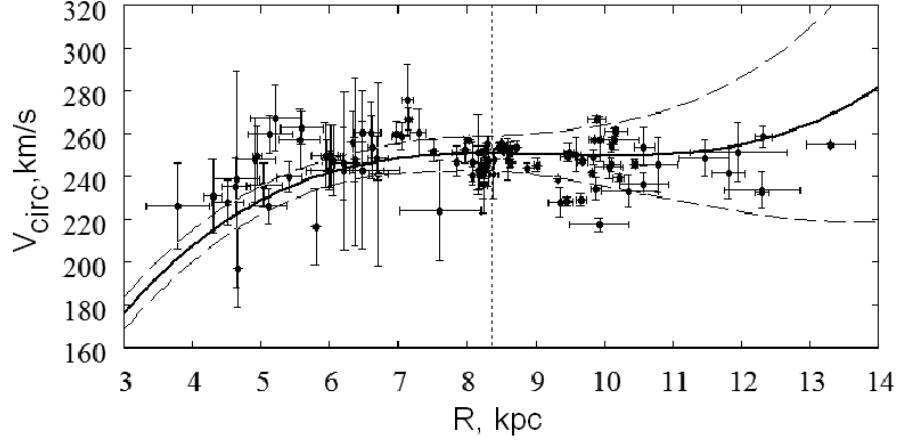


Figure 1: Galactic rotation curve constructed with parameters (9); the thin lines mark the  $1\sigma$  confidence region, the vertical dashed line marks the Sun's position found.

kpc (53 sources) using the weights described above:

$$\begin{aligned}
u_{\odot} &= 10.3 \pm 1.4 \text{ km s}^{-1}, \\
v_{\odot} &= 15.9 \pm 1.4 \text{ km s}^{-1}, \\
w_{\odot} &= 8.1 \pm 1.0 \text{ km s}^{-1}, \\
A &= 16.46 \pm 0.74 \text{ km s}^{-1} \text{ kpc}^{-1}, \\
B &= -15.48 \pm 0.80 \text{ km s}^{-1} \text{ kpc}^{-1}, \\
F &= -3.81 \pm 0.96 \text{ km s}^{-1} \text{ kpc}^{-2}, \\
A^{\circ}/R_0 &= 1.97 \pm 0.36 \text{ km s}^{-1} \text{ kpc}^{-2},
\end{aligned} \tag{11}$$

then

$$\begin{aligned}
\omega_0 &= -31.94 \pm 1.09 \text{ km s}^{-1} \text{ kpc}^{-1}, \\
\omega'_0 &= 3.95 \pm 0.18 \text{ km s}^{-1} \text{ kpc}^{-2}, \\
\omega''_0 &= -0.91 \pm 0.23 \text{ km s}^{-1} \text{ kpc}^{-3}, \\
R_0 &= 8.33 \pm 0.38 \text{ kpc},
\end{aligned}$$

with the error per unit weight being  $\sigma_0 = 7.2 \text{ km s}^{-1}$ . In comparison with solutions ((9) and (10), the values of such local parameters as  $w_{\odot}$ ,  $A$  and  $B$ , are determined here slightly better, but the value of  $\omega''_0$  is determined less reliably because of the reduction in the sample radius.

Figure 1 shows an example of the Galactic rotation curve,  $V_{\text{circ}} = |R\omega|$ , constructed with parameters (9), where the velocities of 106 masers are plotted. As can be seen from the figure, the rotation curve describes satisfactorily the distribution of maser rotation velocities in the range  $4 < R < 12 \text{ kpc}$ .

It can be concluded that the method based on the generalized Oort equations yields pretty good results and extends the capabilities of the linear Oort—Lindblad model (which can be used up to distances of 2 kpc) to heliocentric distances of 3—4 kpc, while the main feature of the method is that the distance  $R_0$  can be estimated fairly easily. As we see from the solutions obtained from masers, this distance is  $R_0 = 8.3 \pm 0.4 \text{ kpc}$ .

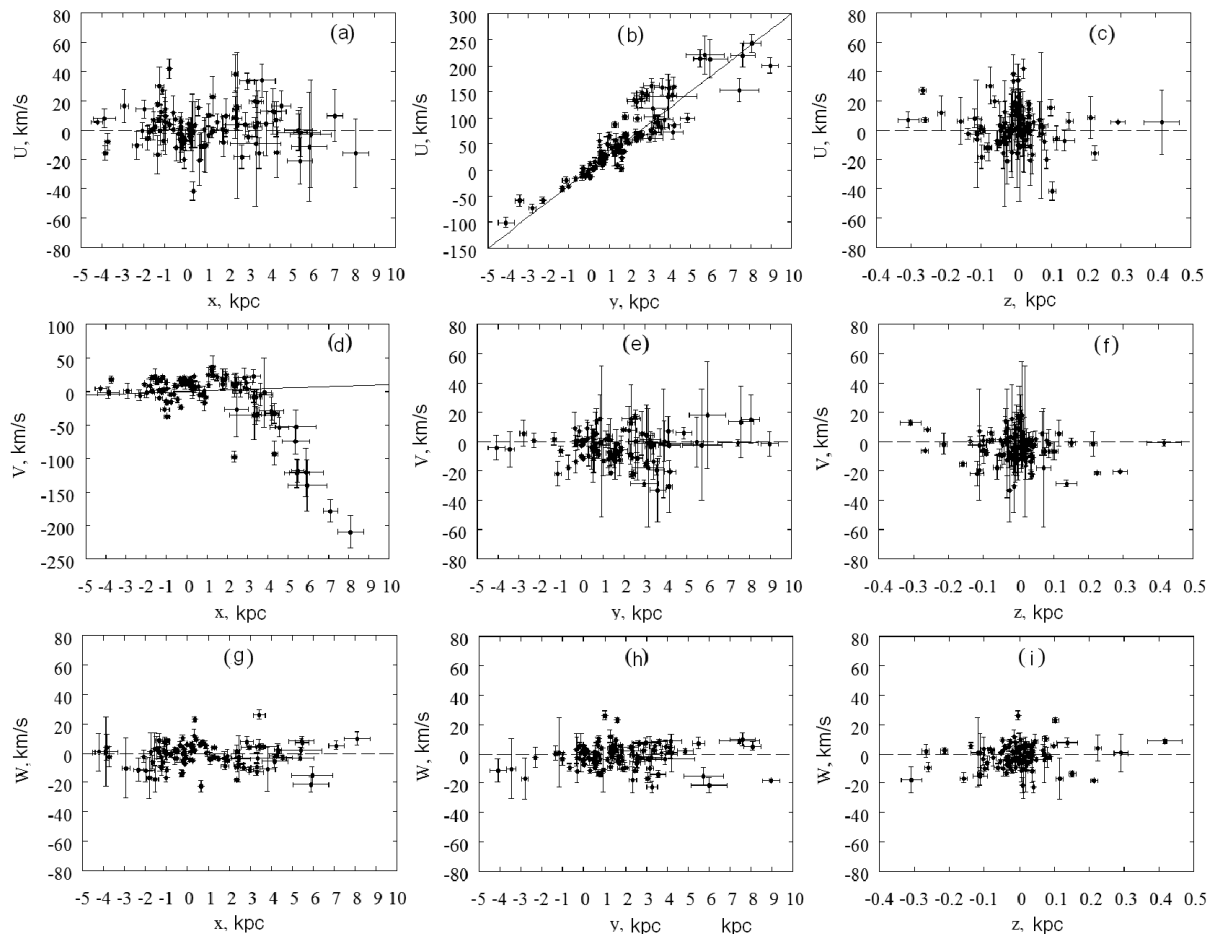


Figure 2: Velocities of the sample of 106 masers versus coordinates. The velocities on panels (b) and (d) are not the residual ones; the velocities  $u$  and  $v$  on the other panels are the residual ones.

Let us now turn to the Ogorodnikov–Milne model. Figure 2 presents nine dependences of the maser velocities  $u, v, w$  on coordinates  $x, y, z$ . In fact, all nine elements of the displacement matrix  $M$  (6) are displayed here graphically, with the panels in the figure following in the same order as the elements of the matrix  $M$  in forms (7) and (8).

The Galactic rotation around the  $z$  axis is described by the velocities  $u$  and  $v$  that lie in the Galactic  $xy$  plane. Four panels, (a), (b), (d), and (e), refer to this motion. The velocities on panels (b) and (d) are not the residual ones, while those on the remaining panels are the residual ones that were formed by taking into account the Galactic rotation with parameters (9) in the velocities  $V_r, V_l$  and  $V_b$ . The thin solid line on panel (b) plots the dependence  $\partial u/\partial y = 30 \text{ km s}^{-1} \text{ kpc}^{-1}$ ; this is the angular velocity of Galactic rotation taken with the opposite sign,  $-\omega_0 = -(B - A) = -V_\theta/R$ . The plotted linear dependence is seen to represent excellently the data in the wide range of the coordinate  $y = [-3; 8] \text{ kpc}$ . This suggests that the term  $\partial V_R/(R\partial\theta)$  in matrix (8) may be set equal to zero. Since there are no significant linear trends on panels (a) and (e), it can be concluded that no large-scale effects like expansion/contraction are present in the Galaxy in the range of distances under consideration. The thin solid line on panel (d) plots the dependence  $\partial v/\partial x = 1 \text{ km s}^{-1} \text{ kpc}^{-1}$ ; this is the first derivative of the linear Galactic rotation velocity,  $A + B = \partial V_\theta/\partial R$ .



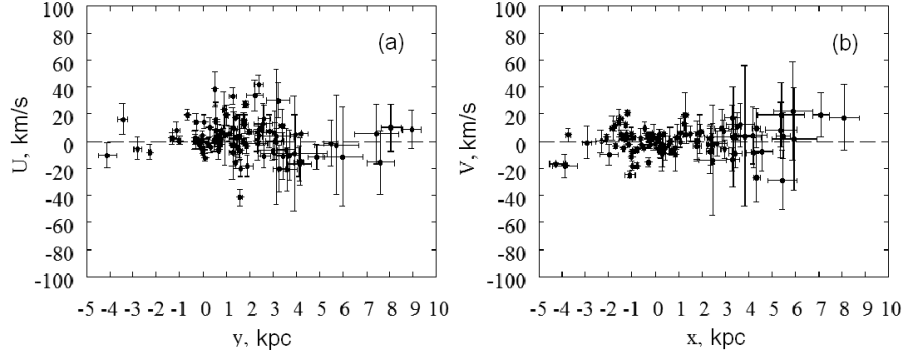


Figure 3: Residual velocities  $u$  and  $v$  of the masers versus coordinates  $y$  and  $x$ , respectively.

The application of the linear approach is clearly seen to be limited by a radius of  $\approx 2$  kpc from the Sun; the velocities  $v$  beyond this range deviate significantly from the linear trend.

Figure 3 presents the dependences of the residual maser velocities  $u$  and  $v$  on coordinates  $y$  and  $x$ , respectively. Allowance for the Galactic rotation parameters (9) found with two derivatives of the angular velocity is seen to correct the data quite well, although a wave with a small amplitude ( $\approx 10 \text{ km s}^{-1}$ ) is visible in the velocities  $u$  on the left panel of Fig.3.

Panels (e), (f), (h), and (i) in Fig.2 refer to the motions in the  $yz$  plane. As we see from the figure, no significant linear trends are traceable here. This plane is interesting in that the velocities of the objects can have a kinematic relationship to such a large scale phenomenon in the Galaxy as the disk warp (Bobylev 2013). The masers at great (more than 10 kpc) heliocentric distances in directions  $l \approx 90^\circ$  and  $l \approx 270^\circ$  with considerable  $z$  are clearly not yet enough to study this effect based on them.

Panels (a), (c), (g), and (i) in Fig.2 refer to the motions in the  $xz$  plane. No significant linear trends are traceable here either. Panel (g), where a periodicity with a wavelength of 3–4 kpc and an amplitude of  $\approx 10 \text{ km s}^{-1}$  is clearly seen, engages our attention. According to the linear model of the spiral structure by Lin and Shu (1964), only the velocities  $V_R$  and  $V_\theta$  are subjected to perturbations from the density wave. Manifestations of these perturbations are clearly seen on panels (a) and (d) in Fig.2 as well as on the right panel in Fig.3.

The tangential velocity perturbations produced by the spiral density wave are clearly seen in Fig.1 as periodic deviations from the smooth rotation curve. They manifest themselves even better in the radial velocities  $V_R$ , which can be easily seen from Fig.4.

Figure 5 shows an example of the influence of the spiral structure on the velocity components  $u$  and  $v$ . The corrections were calculated for each maser with the following model parameters: equal (in magnitude) amplitudes,  $f_R = -8 \text{ km s}^{-1}$  and  $f_\theta = 8 \text{ km s}^{-1}$ , but individual phases of the Sun in the wave,  $(\chi_\odot)_R = -160^\circ$  and  $(\chi_\odot)_\theta = -50^\circ$ , the wavelength  $\lambda = 2.4 \text{ kpc}$ , a two-armed spiral pattern,  $m = 2$ . These parameters of the spiral density wave were found in Bobylev and Bajkova (2013) from masers, where the method of allowance for these perturbations directly in the components  $V_r$ ,  $V_l$ , and  $V_b$  is described in detail.

We can see from the figure that waves are clearly visible in the immediate solar neighborhood on the two left panels ( $u = f(x)$  and  $v = f(x)$ ). Thus, there is no doubt that the periodic velocity perturbations manifesting themselves in Fig.2 (panel (a)) and Fig.3 are related to the influence of the Galactic spiral density wave.

If the periodicity in the velocities  $w$  as a function of  $x$  (Fig.2) is related to the spiral

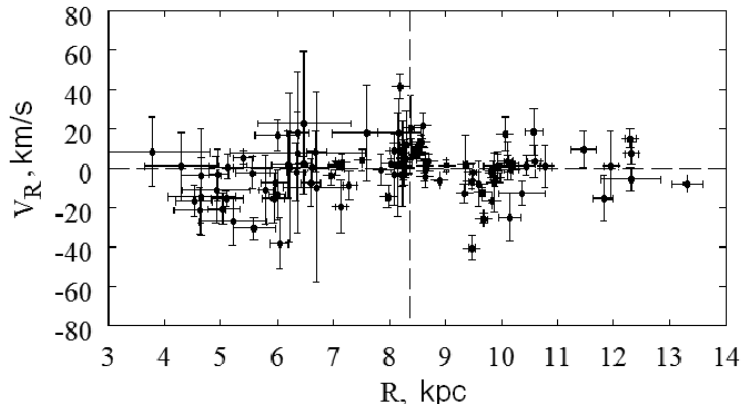


Figure 4: Radial velocity  $V_R$  versus Galactocentric distance  $R$ ; the vertical dashed line marks the Sun's position found.

structure, then the dependence of  $w$  on  $R$  must be more interesting. This dependence is presented in Fig.6. We can see from the figure that the picture is blurred in the inner region of the Galaxy, but the masers in the Local arm and the Perseus arm ( $R \approx 10$  kpc) have significant perturbations. About 30 masers belong to the Local arm. The velocity distribution shown in Fig.6 comes as no surprise for the Gould Belt. Indeed, if the Gould Belt stars are subjected to intrinsic expansion away from the center  $l \approx 180^\circ$  at an angle to the Galactic plane of  $20^\circ$  (Bobylev 2006), then there will be projections of these velocities onto the  $z$  axis. The projections of these velocities will be positive for the stars of the Scorpius–Centaurus association ( $R < R_0$ ) and negative for the stars of the Orion association ( $R > R_0$ ), exactly as in the figure. Remarkably, removing the Gould Belt objects ( $r < 0.5$  kpc) from the sample does not change the picture. Thus, the entire Local arm shows a velocity perturbation in  $z$ , for which a single mechanism, for example, the density wave, can be responsible.

Finally, note the paper by Branham (2014), who analyzed the three-dimensional kinematics of more than 6000 OB stars within  $r < 3$  kpc of the Sun. He used a method based on the generalized Oort formulas, with two more terms having been added to Eqs. (3)–(5):  $\partial w / \partial z$  and  $\partial^2 w / \partial z^2$ . As can be seen on panel (i) in Fig. 2, even the linear trend ( $\partial w / \partial z$ ) is invisible. Therefore, adding these two terms when studying the masers seems inappropriate so far.

## DISCUSSION

Using the generalized Oort formulas, Branham (2014) estimated the solar Galactocentric distance from OB stars to be  $R_0 = 6.72 \pm 0.39$  kpc. This estimate differs noticeably from the estimates of other authors.

Bobylev and Bajkova (2014) applied a method based on Bottlinger's formulas (1) but without expanding Eq. (2) in a series, because  $R$  was calculated directly from this formula using the distances  $r$  to stars. The following solution was obtained from data on 73 masers:  $u_\odot = 7.81 \pm 0.63$  km s $^{-1}$ ,  $v_\odot = 17.47 \pm 0.33$  km s $^{-1}$ ,  $w_\odot = 7.73 \pm 0.23$  km s $^{-1}$ ,  $\omega_0 = -28.86 \pm 0.45$  km s $^{-1}$  kpc $^{-1}$ ,  $\omega'_0 = 3.96 \pm 0.09$  km s $^{-1}$  kpc $^{-2}$ ,  $\omega''_0 = -0.790 \pm 0.027$  km s $^{-1}$

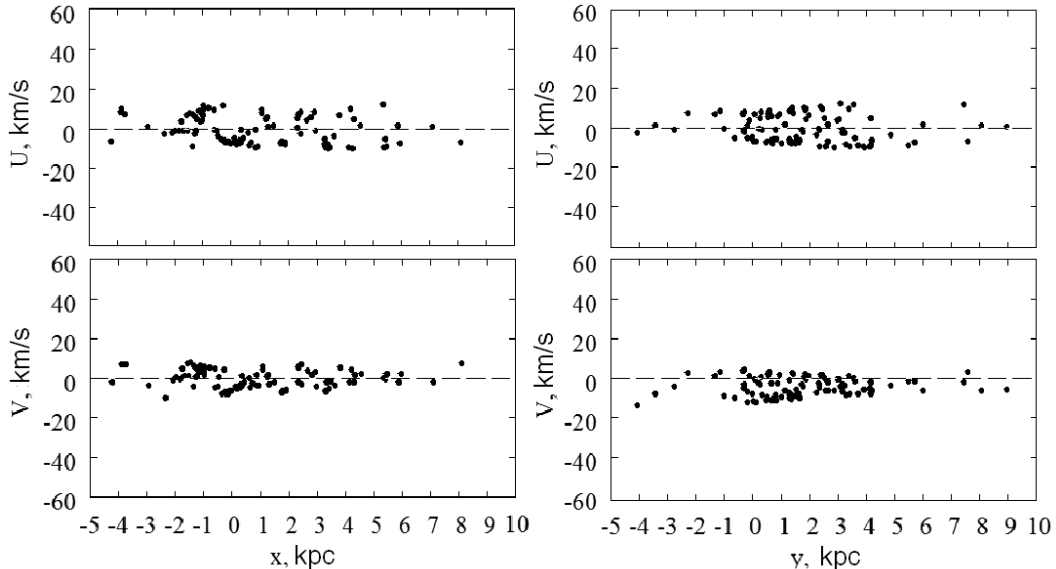


Figure 5: Example of the influence of the spiral structure on the velocity components  $u$  and  $v$  as a function of coordinates  $x$  and  $y$ ; for details, see the text.

$\text{kpc}^{-3}$ ,  $R_0 = 8.3 \pm 0.2 \text{ kpc}$ . In this case, the Oort constants are  $A = 16.49 \pm 0.60 \text{ km s}^{-1} \text{ kpc}^{-1}$  and  $B = -12.37 \pm 1.12 \text{ km s}^{-1} \text{ kpc}^{-1}$ . It can be seen that all parameters are determined in this case with smaller errors than those in solutions (9), (10), or (11), but the  $R_0$  estimation methods differ.

Our new estimate of  $R_0 = 8.3 \pm 0.4 \text{ kpc}$  obtained here is consistent with the results of other authors found by applying different methods based on different data. Some of the results were pointed out in the Introduction. We can point out several more interesting works. Having analyzed the orbits of stars moving around the massive black hole at the Galactic center (the dynamical parallax method), Gillessen et al. (2009) obtained an estimate of  $R_0 = 8.33 \pm 0.35 \text{ kpc}$ . According to VLBI measurements, the radio source Sgr A\* has a proper motion relative to extragalactic sources of  $6.379 \pm 0.026 \text{ mas yr}^{-1}$  (Reid and Brunthaler 2004), using which Schönrich (2012) found  $R_0 = 8.27 \pm 0.29 \text{ kpc}$ . Two  $\text{H}^2\text{O}$  maser sources, Sgr B2N and Sgr B2M, are located in the immediate vicinity of the Galactic center, where the radio source Sgr A\* lies. Based on their direct trigonometric VLBI measurements, Reid et al. (2009b) obtained an estimate of  $R_0 = 7.9_{-0.7}^{+0.8} \text{ kpc}$ . Francis and Anderson (2014) gave a summary of 135 publications devoted to the  $R_0$  determination from 1918 to 2013. They concluded that the results obtained after 2000 give a mean value of  $R_0$  close to  $8.0 \text{ kpc}$ .

The detected oscillations of the velocities  $w$  as a function of  $x$  (panel (g) in Fig.2) or  $R$  (Fig.6) show that beyond-the-model (with respect to the linear Ogorodnikov-Milne model) harmonics in the motion of stars (Vityazev and Tsvetkov 2014) can actually manifest themselves in different planes, but they have the pattern of local perturbations. Obviously, if the sample radius is small, then the amplitude of such local harmonics can be significant. Indeed, if a linear trend is drawn in Fig.6 through the Local arm masers, then a large coefficient  $\partial w / \partial R \approx -22 \text{ km s}^{-1} \text{ kpc}^{-1}$  determined with a small error is obtained.

The perturbations only in the radial and tangential velocities are considered in most models of the Galactic spiral structure. Interestingly, large-scale vertical velocity perturba-

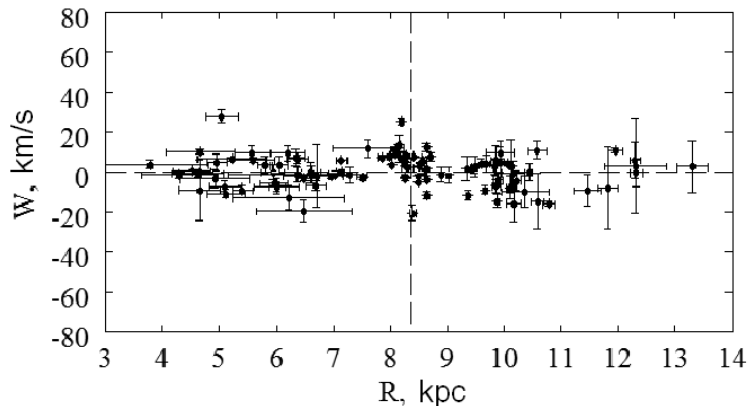


Figure 6: Velocity  $w$  versus Galactocentric distance  $R$ ; the vertical line marks the Sun’s position found.

tions have been found recently in the Galactic disk based on data from several experiments, such as SEGUE (Widrow et al. 2012), RAVE (Williams et al. 2013), and LAMOST (Carlin et al. 2013). The nonzero vertical velocities of objects are usually explained by the action of some external factors, for example, by the passage of a dwarf galaxy or clouds of dark matter through the Galactic disk. However, such perturbations can also be explained without invoking the action of external forces. Small velocity perturbations in the vertical direction can take place within the density wave theory. For example, Fridman (2007) pointed out the possibility of such perturbations. The numerical simulations performed, for example, by Faure et al. (2014) or Debattista (2014) have shown that the propagation of a spiral density wave in the Galactic disk can give rise to vertical oscillations with an amplitude of 10–20  $\text{km s}^{-1}$ .

At present, the observations of  $\approx 400$  masers are being carried out within the framework of the BeSSeL project (Brunthaler et al. 2011) with the goal of determining their trigonometric parallaxes. Therefore, it will soon be possible to study in more detail the above subtle kinematic effects based on a large sample of sources.

## CONCLUSIONS

We gathered information about the coordinates, line-of-sight velocities, proper motions, and trigonometric parallaxes of Galactic masers from published data. Based on these data, we tested a nonlinear model of Galactic rotation using generalized Oort formulas. This model is interesting in that, apart from the rotation parameters  $\omega_0$ ,  $\omega'_0$ , and  $\omega''_0$  it allows the Galactocentric distance of the Sun  $R_0$  to be easily estimated.

Using a sample of masers with parallax errors  $\varepsilon_\pi/\pi < 10\%$ , we found the Galactic rotation parameters and obtained a kinematic estimate of the solar Galactocentric distance,  $R_0 = 8.3 \pm 0.4$  kpc.

Analysis of the three-dimensional kinematics of 106 masers showed significant nonlinearities to be present in the  $xy$  plane (rotation around the Galactic  $z$  axis) due to the peculiarities of the Galactic rotation curve (the existence of high-order derivatives in the expansion of the angular velocity). No distinct linear trends were found in the other two planes,  $xz$  and

*yz*. The presence of a wave in the velocities  $w$  as a function of coordinate  $x$  or  $R$  with a wavelength of  $\approx 3$  kpc and an amplitude of  $10 \text{ km s}^{-1}$  is of considerable interest. This wave is probably associated with the Galactic spiral density wave.

## ACKNOWLEDGMENTS

We are grateful to the referee for the useful remarks that contributed to an improvement of the paper. This work was supported by the “Nonstationary Phenomena in Objects of the Universe” Program P-21 of the Presidium of the Russian Academy of Sciences.

## REFERENCES

1. Y. Asaki, H. Imai, A. M. Sobolev, and S. Yu. Parfenov, arXiv:1404.6947 (2014).
2. V. V. Bobylev, *Astron. Lett.* 32, 816 (2006).
3. V. V. Bobylev, A. T. Bajkova, and S. V. Lebedeva, *Astron. Lett.* 33, 720 (2007).
4. V. V. Bobylev and A. T. Bajkova, *Astron. Lett.* 39, 809 (2013).
5. V. V. Bobylev, *Astron. Lett.* 39, 819 (2013).
6. V. V. Bobylev and A. T. Bajkova, *Astron. Lett.* 40, 389 (2014).
7. R. L. Branham, *Astrophys. Space Sci.* 999, 242 (2014).
8. A. Brunthaler, M. J. Reid, K. M. Menten, X.-W. Zheng, A. Bartkiewicz, Y. K. Choi, T. Dame, K. Hachisuka, K. Immer, G. Moellenbrock, et al., *Astron. Nachr.* 332, 461 (2011).
9. R. A. Burns, Y. Yamaguchi, T. Handa, T. Omodaka, T. Nagayama, A. Nakagawa, M. Hayashi, T. Kamezaki, J. O. Chibueze, et al., arXiv:1404.5506 (2014).
10. J. L. Carlin, J. DeLaunay, H. J. Newberget, L. Deng, D. Gole, K. Grabowski, G. Jin, C. Liu, X. Liu, et al., *Astrophys. J.* 777, L5 (2013).
11. J. O. Chibueze, H. Sakanoue, T. Nagayama, T. Omodaka, T. Handa, T. Kamezaki, R. Burns, H. Kobayashi, H. Nakanishi, M. Honma, et al., arXiv:1406.277 (2014).
12. D. P. Clemens, *Astrophys. J.* 295, 422 (1985).
13. V. Debattista, *Mon. Not. R. Astron. Soc.* 443, L1 (2014).
14. S. Dzib, L. Loinard, A. J. Mioduszewski, A. F. Boden, L. F. Rodriguez, and R. M. Torres, *Astrophys. J.* 718, 610 (2010).
15. C. Faure, A. Siebert, and B. Famaey, *Mon. Not. R. Astron. Soc.* 440, 2564 (2014).
16. T. Foster and B. Cooper, *ASP Conf. Ser.* 438, 16 (2010).
17. C. Francis and E. Anderson, *Mon. Not. R. Astron. Soc.* 441, 1105 (2014).
18. A. M. Fridman, *Phys. Usp.* 50, 115 (2007).
19. S. Gillessen, F. Eisenhauer, S. Trippe, T. Alexander, R. Genzel, F. Martins, and T. Ott, *Astroph. J.* 692, 1075 (2009).
20. T. Hirota, T. Bushimata, Y. K. Choi, M. Honma, H. Imai, K. Iwadate, T. Jike, S. Kamenno, O. Kameya, R. Kamohara, et al., *Publ. Astron. Soc. Jpn.* 59, 897 (2007).
21. T. Hirota, T. Bushimata, Y. K. Choi, M. Honma, H. Imai, K. Iwadate, T. Jike, O. Kameya, R. Kamohara, et al., *Publ. Astron. Soc. Jpn.* 60, 37 (2008).
22. M. Honma, T. Nagayama, K. Ando, T. Bushimata, Y. K. Choi, T. Handa, T. Hirota, H. Imai, T. Jike, et al., *Publ. Astron. Soc. Jpn.* 64, 136 (2012).
23. H. Imai, N. Sakai, H. Nakanishi, H. Sakanoue, M. Honma, and T. Miyaji, *Publ. Astron. Soc. Jpn.* 64, 142 (2012).

24. M. K. Kim, T. Hirota, M. Honma, H. Kobayashi, T. Bushimata, Y. K. Choi, H. Imai, K. Iwadate, T. Jike, S. Kamenno, et al., *Publ. Astron. Soc. Jpn.* 60, 991 (2008).
25. K. Kusuno, Y. Asaki, H. Imai, and T. Oyama, *Astrophys. J.* 774, 107 (2013).
26. E. S. Levine, C. Heiles, and L. Blitz, *Astrophys. J.* 679, 1288 (2008).
27. C. C. Lin and F. H. Shu, *Astrophys. J.* 140, 646 (1964).
28. L. Loinard, R. M. Torres, A. J. Mioduszewski, L. F. Rodriguez, R. A. Gonzalez-Lopezlira, R. Lachaume, V. Vazquez, and E. Gonzalez, *Astrophys. J.* 671, 546 (2007).
29. L. Loinard, R. M. Torres, A. J. Mioduszewski, and L. F. Rodriguez, *Astrophys. J.* 675, 29 (2008).
30. N. M. McClure-Griffiths, and J. M. Dickey, *Astroph. J.* 671, 427 (2007).
31. A. M. Mel'nik, and A. K. Dambis, *Mon. Not. R. Astron. Soc.* 400, 518 (2009).
32. K. F. Ogorodnikov, *Dinamika zvezdnykh sistem* (M.: Fizmatgiz, 1965).
33. M. E. Popova and A. V. Loktin, *Astron. Lett.* 31, 663 (2005).
34. M. J. Reid, *Annu. Rev. Astron. Astrophys.* 31, 345 (1993).
35. M. Reid and A. Brunthaler, *Astroph. J.* 616, 872 (2004).
36. M. J. Reid, K. M. Menten, X. W. Zheng, A. Brunthaler, L. Moscadelli, Y. Xu, B. Zhang, M. Sato, M. Honma, T. Hirota, et al., *Astrophys. J.* 700, 137 (2009a).
37. M. Reid, K. M. Menten, X. W. Zheng, A. Brunthaler, and Y. Xu, *Astrophys. J.* 705, 1548 (2009b).
38. M. J. Reid, J. E. McClintock, R. Narayan, L. Gou, R. A. Remillard, and J. A. Orosz, *Astrophys. J.* 742, 83 (2011).
39. M. J. Reid, K. M. Menten, A. Brunthaler, X.W. Zheng, T.M. Dame, Y. Xu, Y.Wu, B. Zhang, A. Sanna, M. Sato, et al., *Astrophys. J.* 783, 130 (2014).
40. K. L. J. Rygl, A. Brunthaler, M. J. Reid, K. M. Menten, H. J. van Langevelde, and Y. Xu, *Astron. Astrophys.* 511, A2 (2010).
41. R. Schöomrich, *Mon. Not. R. Astron. Soc.* 427, 274 (2012).
42. R. M. Torres, L. Loinard, A. J. Mioduszewski, and L. F. Rodriguez, *Astrophys. J.* 671, 1813 (2007).
43. R. M. Torres, L. Loinard, A. J. Mioduszewski, and L. F. Rodriguez, *Astrophys. J.* 698, 242 (2009).
44. R. M. Torres, L. Loinard, A. J. Mioduszewski, A. F. Boden, R. Franco-Hernandez, W. H. T. Vlemmings, and L. F. Rodriguez, *Astrophys. J.* 747, 18 (2012).
45. V. V. Vityazev and A. S. Tsvetkov, *Mon. Not. R. Astron. Soc.* 442, 1249 (2014).
46. L. M. Widrow, S. Gardner, B. Yanny, S. Dodelson, and H.-Yu. Chen, *Astrophys. J.* 750, L41 (2012).
47. M. E. K. Williams, M. Steinmetz, J. Binney, A. Siebert, H. Enke, B. Famaey, I. Minchev, R. S. de Jong, C. Boeche, K. C. Freeman, et al., *Mon. Not. R. Astron. Soc.* 436, 101 (2013).
48. M. V. Zabolotskikh, A. S. Rastorguev, and A. K. Dambis, *Astron. Lett.* 28, 454 (2002).
49. J. Ziolkowski, *Mon. Not. R. Astron. Soc.* 358, 851 (2005).